Supporting Information

Lemoine et al. 10.1073/pnas.1318715110

SI Materials and Methods

Chemical Synthesis. All chemicals were purchased from Sigma-Aldrich or Alfa Aesar in analytical grade. An Agilent 6975 MSD was used for electrospray ionization (ESI) analysis. ^{1}H-NMR and ^{13}C-NMR were run at 300 or 400 and 75 or 100 MHz, respectively. Coupling constants (*J*) are quoted in hertz (Hz) and chemical shifts (δ) are given in parts per million (ppm) using the residue solvent peaks as reference relative to tetramethylsilane (TMS); s is singlet, d is doublet, t is triplet, q is quadruplet, m is multiplet. A Beta-Basic C^{18} column from Thermo Scientific (10 × 250 mm) was used for HPLC semipreparative purifications. Synthesis of maleimide ethylene azobenzene trimethyl ammonium (MEA-TMA), maleimide ethylene azobenzene triethyl ammonuim (MEA-TEA), maleimide azobenzene quaternary ammonium (MAQ), MEA-SO_3, and MEA-OMe was carried out as follows.

(E)-*N*-(4-((4-aminophenyl)diazenyl)phenyl)-3-(2,5-dioxo-2,5-dihydro-1*H*-pyrrol-1-yl)propanamide **S1a**: O-Benzotriazole-*N*,*N*,*N*',*N*'-tetramethyl-uronium-hexafluoro-phosphate (HBTU) (893 mg, 2.36 mmol) was added to a solution of (3-(2,5-dioxo-2,5-dihydro-1*H*-pyrrol-1-yl)propanoic acid (399 mg, 2.36 mmol), which was obtained as described previously (1), 4-[(E)-2-(4-aminophenyl)diazen-1-yl]aniline (417 mg, 1.96 mmol) and triethylamine (0.327 mL, 238 mg, 2.36 mmol) in 10 mL of MeCN. The reaction was carried out for 19 h under argon atmosphere at room temperature. The solution was concentrated in vacuo, dissolved in AcOEt (150 mL), quenched with 150 mL of saturated $NaHCO_3$aq, then extracted with AcOEt (2 × 150 mL). The crude product was purified by column chromatography on silica (heptane/EtOAc, 1/1–2/8 in vol), resulting in the desired orange solid (392 mg, 1.08 mmol, 55%). TLC (EtOAc/heptane, 7/3): Rf = 0.34; ^{1}H-NMR (400 MHz, DMSO - d_6): δ 10.23 (s, H), 7.70 (s, 2H), 7.62 (d, *J* = 8,7 Hz, 4H), 7.04 (s, 2H), 6.67(d, *J* = 8.7 Hz, 2H), 6.02 (s, 2H), 3.74 (t, J^3 = 7.2 Hz, 2H), 2.63 (t, J^3 = 7.2 Hz, 2H); ^{13}C-NMR (100 MHz, Acetone - d_6): δ = 171.38, 169.37, 155.63, 152.86, 149.72, 145.08, 135.26, 125.65, 123.52, 120.30, 114.65, 42.07, 41.34; MS (ESI) (*m*/*z*): $[M+H]^+$ calculated for $C_{19}H_{18}N_5O_3$ 364.14; found, 364.2.

(*E*)-*N*-(4-((4-aminophenyl)diazenyl)phenyl)-2-(2,5-dioxo-2,5-dihydro-1*H*-pyrrol-1-yl)acetamide **S1b**: The **S1b** orange solid (480 mg, 1.37 mmol, 70%) was obtained from 2-(2,5-dioxo-2,5-dihydro-1*H*-pyrrol-1-yl)acetic acid (365 mg, 2.36 mmol), which was obtained as described previously (1), using the same method as with **S1a.** TLC (EtOAc/heptane, 7/3): Rf = 0.35; ^{1}H-NMR (400 MHz, Acetone - d_6): δ 9.77 (s, 1H), 7.79 (s, 4H), 7.72 (d, *J* = 8.8 Hz, 2H), 7.00 (s, 2H), 6.79 (d, *J* = 8.8 Hz, 2H), 4.40 (s, 2H); ^{13}C-NMR (100 MHz, DMSO - d_6): δ 171.16, 165.08, 153.02, 148.84, 143.32, 140.07, 135.47, 125.37, 123.05, 119.94, 113.90, 38.73; MS (ESI) (*m*/*z*): $[M+H]^+$ calculated for $C_{18}H_{16}N_5O_3$ 350.12; found, 350.

(*E*)-2-((4-((4-(3-(2,5-dioxo-2,5-dihydro-1*H*-pyrrol-1-yl)propanamido)phenyl)diazenyl)phenyl)amino)-*N*,*N*,*N*-trimethyl-2-oxoethanaminium 2,2,2-trifluoroacetate **MEA-TMA (1a)**: 1-carboxy-*N*,*N*,*N*-trimethylmethanaminium chloride (74 mg, 0.48 mmol) was dissolved in 10 mL of anhydrous DMF. Then, oxalyle chloride (35 mL, 0.48 mmol) was added under argon atmosphere at room temperature. After 2 h, at this temperature, a solution of **S1a** (106 mg, 0.29 mmol) and DIPEA (0.153 mL, 0.88 mmol) in 10 mL of anhydrous DMF was added. The mixture was allowed to stir 19 h at room temperature. Concentration in vacuo afforded a thick orange solid, which was diluted with water (50 mL) and then washed with AcOEt (3 × 50 mL). The aqueous phase was concentrated and purified by semipreparative reverse-phase HPLC using an isocratic elution mode of H_2O (with 0.1% TFA)/MeCN, 75/25 (vol/vol) resulting in the desired orange solid (retention time 10.3 min, 113 mg, 0.196 mmol, 67%). ^{1}H-NMR (400 MHz, D_2O): δ 10.91 (s, 1H), 10.40 (s, 1H), 7.86 (m, 8H), 7.04 (s, 2H), 4.38 (s, 2H), 3.74 (t, *J* = 7.3 Hz, 2H), 3.31 (s, 9H), 2.67 (t, *J* = 7.3 Hz, 2H). MS (ESI) (*m*/*z*): $[M]^+$ calcd for $C_{24}H_{27}N_6O_4$ 463.21; found, 463.20; UV/Vis: λ_{max} 365 nm.

(*E*)-2-((4-((4-(3-(2,5-dioxo-2,5-dihydro-1*H*-pyrrol-1-yl)propanamido)phenyl)diazenyl)phenyl)amino)-*N*,*N*,*N*-triethyl-2-oxoethanaminium 2,2,2-trifluoroacetate **MEA-TEA, 2a**: The **2a** orange solid (51.1 mg, 0.083 mmol, 49%) was obtained after semipreparative reverse-phase HPLC using an isocratic elution mode of H_2O (with 0.1% TFA)/MeCN, 68/32 (vol/vol) (retention time 9.3 min) with *N*-(carboxymethyl)-*N*-ethyl-*N*-methylethanaminium bromide (2) (75 mg, 0.33 mmol), oxalyle chloride (29 μL, 0.33 mmol), **S1a** (60 mg, 0.165 mmol), and DIPEA (110 μL, 0.66 mmol) using the same method as with **1a.** ^{1}H-NMR (400 MHz, MeOD - d_4): δ 7.92 (d, *J* = 9.0 Hz, 2H), 7.87 (d, *J* = 9.0 Hz, 2H), 7.79, (d, *J* = 8.2 Hz, 2H), 7.72 (d, *J* = 8.2 Hz, 2H), 6.83 (s, 2H), 4.20 (s, 2H), 3.69 (q, *J* = 8.0 Hz, 6H), 3.65 (t, *J* = 7.3 Hz, 2H), 2.71 (t, *J* = 7.3 Hz, 2H), 1.40 (t, *J* = 8.0 Hz, 9H). MS (ESI) (*m*/*z*): $[M]^+$ calculated for $C_{27}H_{33}N_6O_4$ 505.26; found, 505.2; UV/Vis: λ_{max} 365 nm.

(*E*)-2-((4-((4-(2-(2,5-dioxo-2,5-dihydro-1*H*-pyrrol-1-yl)acetamido)phenyl)diazenyl)phenyl)amino)-*N*,*N*,*N*-triethyl-2-oxoethanaminium 2,2,2-trifluoroacetate **MAQ (2b)**: The **2b** orange solid (39 mg, 0.065 mmol, 32%) was obtained after semipreparative reverse-phase HPLC using an isocratic elution mode of H_2O (with 0.1% TFA)/MeCN, 68/32 (vol/vol) (retention time 8.6 min) with *N*-(carboxymethyl)-*N*-ethyl-*N*-methylethanaminium bromide (2) (90 mg, 0.40 mmol), oxalyle chloride (34 μL, 0.40 mmol), **S1b** (70 mg, 0.20 mmol), and DIPEA (140 μL, 0.80 mmol) using the same method as with **1a.** ^{1}H-NMR (400 MHz, MeOD - d_4): δ 7.90 (m, 4H), 7.77 (d, *J* = 8.4 Hz, 2H), 7.73 (d, *J* = 8.4 Hz, 2H), 6.94 (s, 2H), 4.38 (s, 2H), 4.19 (s, 2H), 3.68 (q, *J* = 7.0 Hz, 6H), 1.39 (t, *J* = 8.0 Hz, 9H). MS (ESI) (*m*/*z*): $[M]^+$ calculated for $C_{26}H_{31}N_6O_4$ 491.24; found, 491.2; UV/Vis: λ_{max} 365 nm.

(*E*)-2-((4-((4-(3-(2,5-dioxo-2,5-dihydro-1*H*-pyrrol-1-yl)propanamido)phenyl)diazenyl)phenyl)amino)-2-oxoethanesulfonate **MEA-SO_3 (3a): S1a** (135 mg, 0.365 mmol), 2-sulfoacetic acid (56 mg, 0.40 mmol) benzotriazol-1-yl-oxytripyrrolidinophosphonium hexafluorophosphate (PyBOP) (228 mg, 0.438 mmol) and DIPEA (178 μL, 1.023 mmol) were dissolved in 10 mL of anhydrous DMF under argon atmosphere at room temperature. The mixture was allowed to stir 19 h at room temperature. Concentration in vacuo afforded a thick orange solid, which was diluted with water (50 mL) and then washed with AcOEt (3 × 50 mL). The aqueous phase was concentrated and purified by semipreparative reverse-phase HPLC using an isocratic elution mode of H_2O (with 0.1% TFA)/MeCN, 80/20 (vol/vol) resulting in the desired orange solid (retention time 14.2 min, 120 mg, 0.247 mmol, 68%). ^{1}H-NMR (400 MHz, MeOD - d_4): δ 7.86 (m, 4H), 7.79 (d, *J* = 8.8 Hz, 2H), 7.70 (d, *J* = 8.8 Hz, 2H), 6.83 (s, 2H), 3.89 (m, 4H), 2.70 (t, *J* = 7.2 Hz, 2H). MS (ESI) (*m*/*z*): $[M]^-$ calculated for $C_{21}H_{18}N_5O_7S$ 484.09; found, 484.0; UV/Vis: λ_{max} 365 nm.

(*E*)-3-(2,5-dioxo-2,5-dihydro-1*H*-pyrrol-1-yl)-*N*-(4-((4-(2-methoxyacetamido)phenyl)diazenyl)phenyl)propanamide **MEA-OMe (4a)**: **S1a** (32 mg, 0.089 mmol), methoxyacetic acid (9 μL, 0.116 mmol) HBTU (40 mg, 0.107 mmol) and triethylamine (15 μL, 0.107 mmol) were dissolved in 10 mL of anhydrous acetonitrile under argon atmosphere at room temperature. The mixture was allowed to stir 19 h at room temperature. The solution was concentrated in vacuo, dissolved in AcOEt (150 mL), quenched with 150 mL of saturated $NaHCO_3$aq, then extracted with AcOEt (2 × 150 mL). The crude

product was purified by semipreparative reverse-phase HPLC using an isocratic elution mode of H_2O (with 0.1% TFA)/MeCN, 68/32 (vol/vol) resulting in the desired orange solid (retention time 12.1 min, 35 mg, 0.08 mmol, 90%). ^{1}H-NMR (400 MHz, Acetone-d_6): δ 10.34 (s, 1H), 10.10 (s, 1H), 7.85 (m, 8H), 7.04 (s, 2H), 3.74 (t, J =7.3 Hz, 2H), 3.40 (s, 3H), 2.65 (t, J = 7.3 Hz, 2H). MS (ESI) (m/z): $[M-H]^-$ calculated for $C_{22}H_{20}N_5O_5$ 434.15; found, 434.0; UV/Vis: λ_{max} 365 nm.

Relative Permeability Measurements. An agar bridge containing 3 M KCl connected the bath and indifferent electrode. The intracellular (pipette) solution comprised 147 mM NaCl, 10 mM EGTA, 10 mM Hepes, adjusted to pH 7.3 with NaOH, or 140 mM CsCl, 5 mM $MgCl_2$, 5 mM EGTA, 10 mM Hepes, adjusted to pH 7.3 with CsOH. The standard extracellular solution was changed to symmetrical NaCl external solution that contained 147 NaCl, 0.3 mM $CaCl_2$, 13 mM glucose, 10 mM Hepes, adjusted to pH 7.3 with NaOH, and a voltage ramp pulse (from −120 to 120 mV; 200-ms duration) was applied. The solution was then exchanged with one of the following solutions, and another voltage ramp was applied: mannitol (Man) solution, in which most NaCl was replaced by mannitol to maintain osmolarity contained 40 mM NaCl, 0.3 mM $CaCl_2$, 200 mM mannitol, 13 mM glucose, 10 mM Hepes, adjusted to pH 7.3 with NaOH; sodium isethionate solution (Na-Ise) contained 10 mM NaCl, 137 sodium isethionate, 0.3 mM $CaCl_2$, 13 mM glucose, 10 mM Hepes, adjusted to pH 7.3 with NaOH; $CaCl_2$ (Ca) solution contained 110 mM $CaCl_2$, 3 mM glucose, 10 mM Hepes, adjusted to pH 7.3 with $Ca(OH)_2$, and *N*-methyl-D-glucamine (NMDG) solution contained 149 mM NMDG, 0.3 mM $CaCl_2$, 13 mM glucose, 10 mM Hepes, adjusted to pH 7.3 with HCl. For NMDG, voltage ramps were applied 3, 30, and 60 s after light-switching (light intensity for 525 nm was 4.5 mW/mm^2) or ATP (100 μM) application. For light-gated currents, we calculated reversed potential (E_{rev}, mV) from voltage ramps after subtracting photocurrents obtained at 525-nm light to those recorded at 365-nm light. Similarly, for ATP-gated currents, E_{rev} was determined after subtracting currents evoked by ATP [at the indicated concentration, and for the Ca solution 300 μM was used to account for the decreased ATP potency (3)] at 365-nm light to basal currents recorded at the same wavelength in the absence of ATP. Values of E_{rev} were then corrected for liquid junction potentials, which were calculated using IGOR PRO (v6.22A), and used to determine permeability ratios ($P_X/P_{cations}$) as follows: For low NaCl concentration solution, $P_{Cl}/P_{Na} = ([Na]_o \times \exp(-x) - [Na]_i)(1 - \exp(x))/ ([Cl]_i - [Cl]_o \times \exp(x))(1 - \exp(-x))$, where $x = \Delta E_{rev} \times 10^{-3} \times F/RT$ (ΔE_{rev} is the difference between E_{rev} measured in solution for a specific ion X and E_{rev} measured in symmetrical NaCl solution, F is Faraday constant, R is the gas constant, and T is the absolute temperature), $[Na]_o = 44$, $[Na]_i = 157$, $[Cl]_o = 41$, and $[Cl]_i = 147$ mM. In these conditions, the theoretical E_{rev} value for chloride-impermeable channels would be −32 mV. For $CaCl_2$ solution, $P_{Ca}/P_{Na} = ([Na]_i \times \exp(x))(1 + \exp(x))/(4 \times [Ca]_o)$, where $[Na]_i = 157$, and $[Ca]_o = 112$ mM. For the NMDG solution, $P_{NMDG}/P_{Cs} = ([Cs]_i \times \exp(x))/[NMDG]_o$, where $[Cs]_i = 148$, and $[NMDG]_o = 147$ mM. Ion concentrations were converted to activities using the following coefficients: $\gamma_{Na} = 0.75$, $\gamma_{Cl} = 0.75$, $\gamma_{Ca} = 0.28$, $\gamma_{Cs} = 0.75$, $\gamma_{NMDG} = 0.81$. The E_{rev} shown in Fig. 5, and Figs. S5 and S6 are raw data without the correction of junction potential.

1. Allen VC, Robertson CC, Turega SM, Philp D (2010) A simple network of synthetic replicators can perform the logical OR operation. *Org Lett* 12(9):1920–1923.
2. Ōkawa H, et al. (2013) Proton-conductive magnetic metal-organic frameworks, NR3(CH2COOH)[M(a)(II)M(b)(III)(ox)3]: Effect of carboxyl residue upon proton conduction. *J Am Chem Soc* 135(6):2256–2262.
3. Migita K, Haines WR, Voigt MM, Egan TM (2001) Polar residues of the second transmembrane domain influence cation permeability of the ATP-gated P2X(2) receptor. *J Biol Chem* 276(33):30934–30941.

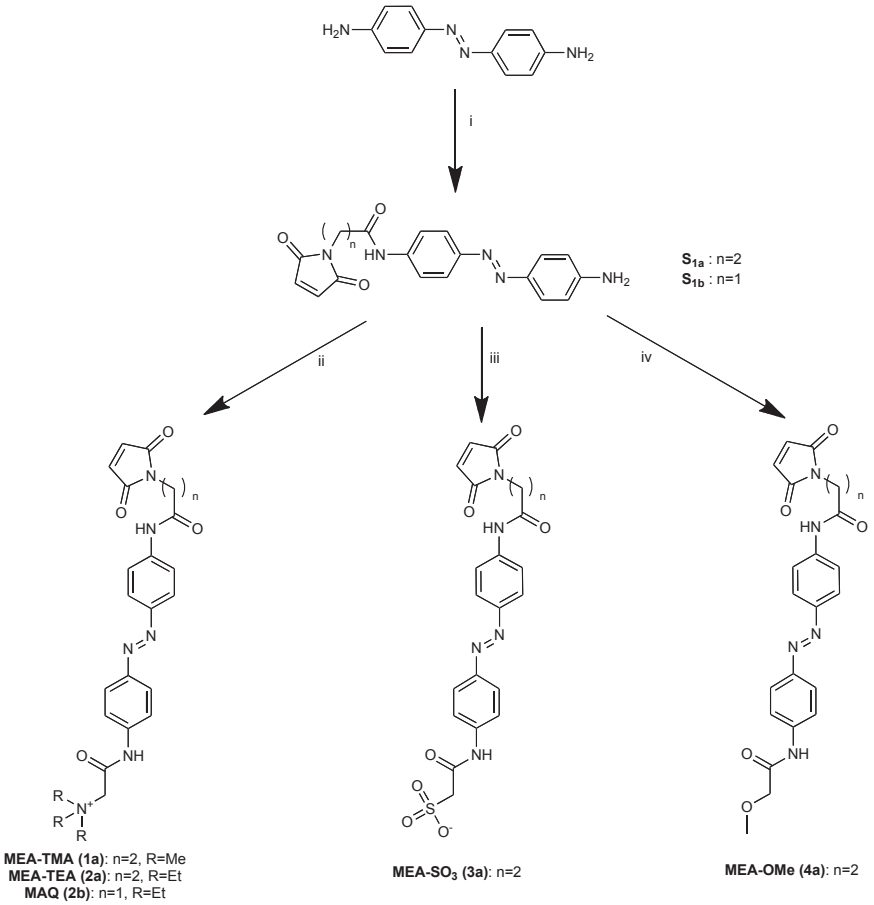

Fig. S1. Synthesis of MEA-TMA, MEA-TEA, MAQ, MEA-SO_3 and MEA-OMe. (*i*) HBTU, Et_3N, (3-(2,5-dioxo-2,5-dihydro-1*H*-pyrrol-1-yl)propanoic acid or 2-(2,5-dioxo-2,5-dihydro-1*H*-pyrrol-1-yl)acetic acid, MeCN, 19 h, room temperature, ρ = 55–70%; (*ii*) 1-carboxy-*N*,*N*,*N*-trimethylmethanaminium chloride or *N*-(carboxymethyl)-*N*-ethyl-*N*-methylethanaminium bromide, oxalyle chloride, DMF, 2 h, room temperature; **S1a** or **S1b**, DIPEA, DMF, 19 h, room temperature, ρ = 32–67%; (*iii*) 2-sulfoacetic acid, PyBOP, DIPEA, DMF, 19 h, room temperature, ρ = 68%; (*iv*) methoxyacetic acid, HBTU, Et_3N, MeCN, 19 h, room temperature, ρ = 90%.

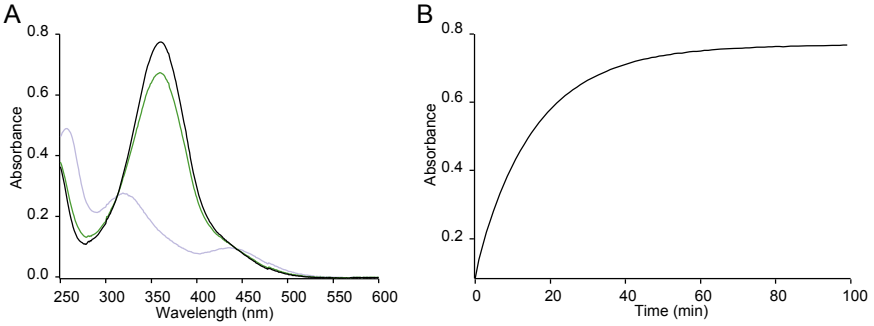

Fig. S2. Kinetics of azobenzene isomerization measured in free solution. (*A*) Absorbance spectra of MEA-TMA recorded: (*i*) in standard extracellular solution in the dark (black trace), (*ii*) following 365-nm light illumination for 3 min (violet trace), and (*iii*) after 525-nm irradiation for 3 min (green trace). (*B*) Thermal relaxation, recorded at 360 nm, of *cis*–MEA-TMA in standard extracellular solution fitted with a single exponential decay function (τ = 16.3 ± 0.9 min, *n* = 3, mean ± SEM).

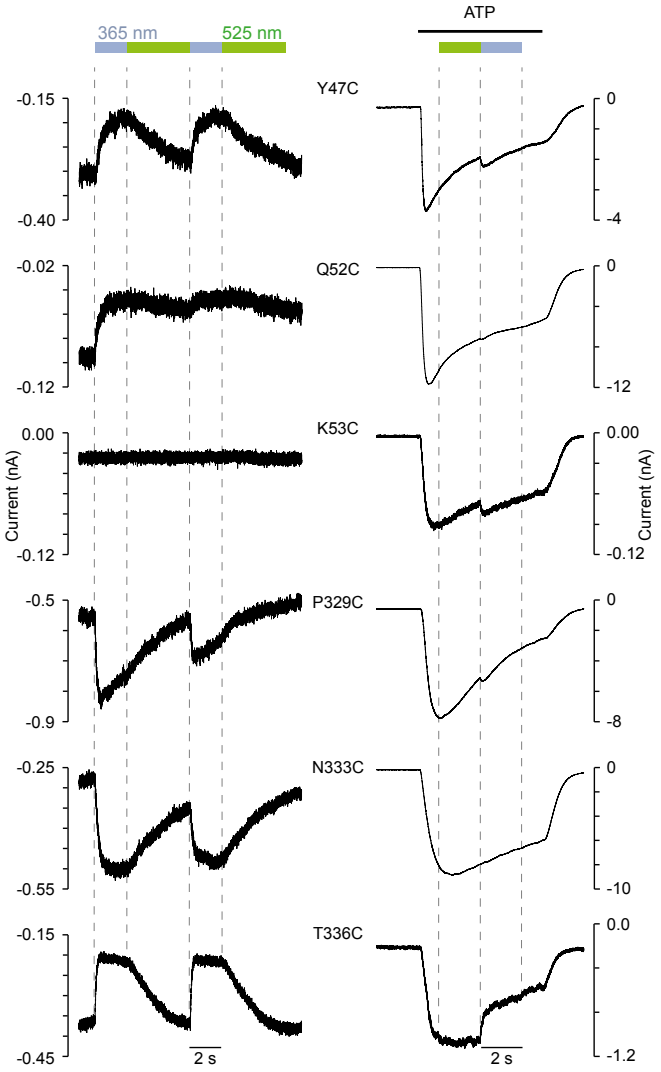

Fig. S3. Tethered MEA-TMA turns on and off the P2X2 channel by light. Whole-cell currents evoked by light or ATP (EC_{50}) in cells expressing the indicated constructs that were prior-treated to MEA-TMA in the dark. Currents were recorded from the same cells. To switch off channels that opened in visible light (for Y47C, Q52C, and T336C mutants), cells were first irradiated with a short 4-s lasting pulse of 365-nm light before ATP application. For Q52C, K53C, N333C, and T336C mutants, labeling was performed in the presence of ATP.

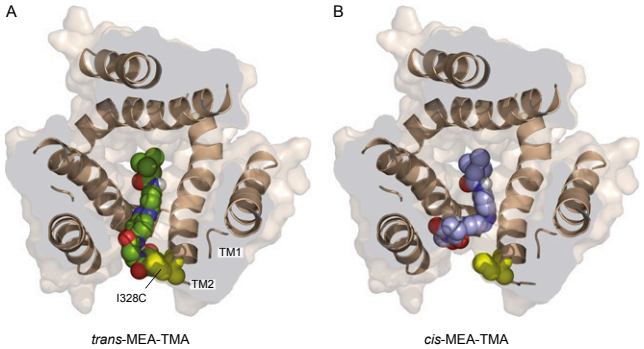

Fig. S4. Docking of MEA-TMA in the rat P2X2 I328C mutant model built from the X-ray structure of the zebrafish P2X4 receptor solved in an ATP-bound, open-channel state. (*A*) The *trans*-isomer spans the distance between the I328C mutation (as indicated in yellow) and the central threefold axis of symmetry where ions are thought to flow. (*B*) The *cis*-isomer, which is shorter than the *trans* one, cannot span this distance, suggesting that once attached to the cysteine, the quaternary ammonium TMA cannot reach the central axis necessary for efficient blockage.

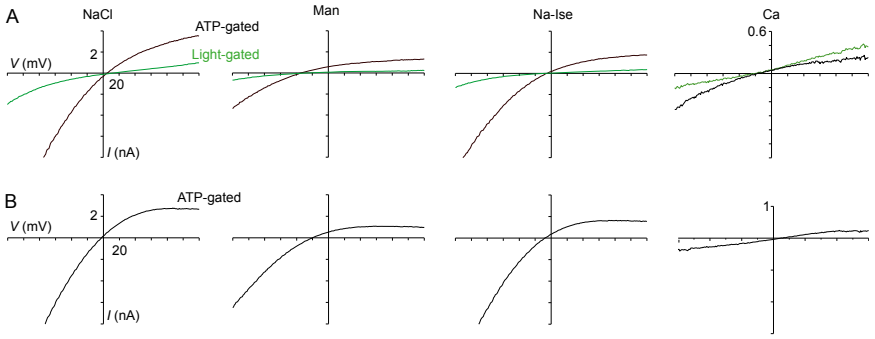

Fig. S5. Light-gated P2X2 receptor is permeable to sodium and calcium ions but not to chloride ions. (*A*) Current-voltage curves for ATP-gated (3 μM or 300 μM for Ca solution) (black) or light-gated (525 nm) (green) currents recorded in HEK cells expressing the I328C mutant tethered to MEA-TMA in different extracellular solutions. Light-gated currents were obtained after subtracting photocurrents recorded at 525-nm light to those obtained at 365-nm light. ATP-gated currents were obtained after subtracting ATP currents recorded at 365-nm light to basal currents recorded at the same wavelength (*Materials and Methods*). (*B*) Current-voltage curves for ATP (10 μM or 300 μM for Ca solution)-gated currents recorded in HEK cells expressing the P2X2-3T receptor at the indicated extracellular solutions as shown in *A*.

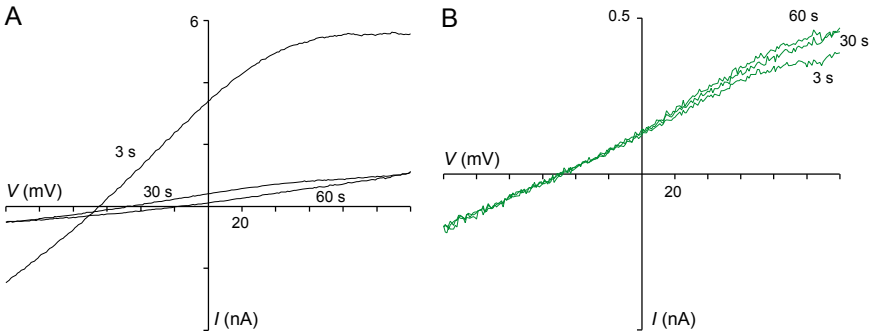

Fig. S6. Light-gated P2X2 receptors display small permeability to NMDG ions. (*A*) Current-voltage curves for ATP-gated (100 μM) currents recorded in NMDG solution at the indicated time after ATP application, in a HEK cell expressing the P2X2-3T receptor. (*B*) Current-voltage curves for light-gated (current at 525 nm subtracted from that at 365 nm) currents recorded at the same times as those shown in *A* after light-switching, in a HEK cell expressing the I328C mutant tethered to MEA-TMA.

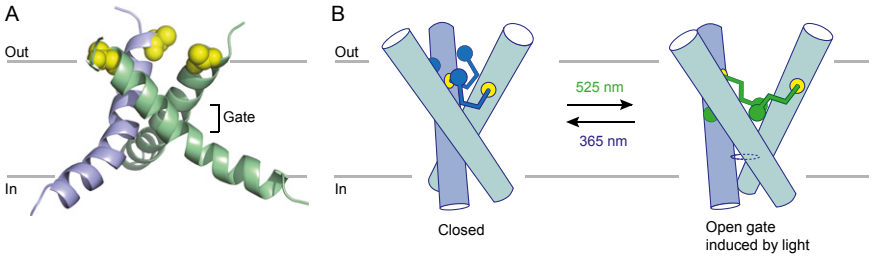

Fig. S7. Proposed light-induced gating mechanism at position I328. (*A*) Lateral view of the P2X4 channel from the crystal structure solved in the closed state (PDB ID code 4DW0). The gate is formed by tight association of the three transmembrane (TM) 2 α-helices from each subunit that are steeply angled (about 50°) relative to the normal of the membrane plane. For clarity, TM1 segments were removed and residue I336, which is homologous to the P2X2 I328 is highlighted in yellow. (*B*) Scheme illustrating for the P2X2 receptor the proposed mechanism in which isomerization of photoswitches tethered to I328C (yellow) forces adjacent TM2 α-helices to move apart, causing pore expansion. For clarity, three attached MEA-TMA molecules are shown, but no assumption on labeling stoichiometry is made. The view is similar to that shown in *A*.

Table S1. Characterization and screening of P2X2 single cysteine mutants with MEA-TMA

Constructs	ATP EC_{50} (μM)	n_H	Dark (pA/pF)	365 nm (pA/pF)	525 nm (pA/pF)	$\tau_{365\ nm}$ (s)	$\tau_{525\ nm}$ (s)
P2X2-3T	15.0 ± 2.0	2.9 ± 0.5	−5.0 ± 1.8	−5.8 ± 1.9	−5.9 ± 1.9	—	—
F44C	1.1 ± 0.4	1.3 ± 0.2	−21.1 ± 4.5	−22.3 ± 4.6	−22.9 ± 4.8	—	—
V45C	9.7 ± 0.8	1.6 ± 0.4	−3.6 ± 0.5	−4.0 ± 0.6	−4.5 ± 0.5	—	—
W46C	12.4 ± 3.1	1.8 ± 0.4	−4.2 ± 1.6	−4.9 ± 1.7	−5.4 ± 1.8	—	—
Y47C	2.5 ± 0.9	1.1 ± 0.1	−17.0 ± 2.9	−13.0 ± 2.1	−18.4 ± 3.0	0.253 ± 0.027	2.774 ± 0.115
V48C	9.4 ± 4.7	1.6 ± 0	−47.0 ± 5.6	−116.7 ± 13.9	−47.3 ± 5.6	0.335 ± 0.037	3.127 ± 0.200
F49C	6.8 ± 0.9	1.6 ± 0.3	−4.8 ± 0.7	−5.1 ± 0.6	−5.5 ± 0.6	—	—
I50C	15.6 ± 2.6	1.8 ± 0.4	−14.1 ± 5.7	−14.8 ± 5.8	−15.5 ± 5.6	—	—
V51C	32.8 ± 6.6	1.5 ± 0.2	−3.4 ± 0.7	−4.3 ± 0.8	−4.2 ± 0.8	—	—
Q52C	93.9 ± 13.8	1.7 ± 0.1	−7.7 ± 1.2	−4.7 ± 0.8	−8.6 ± 1.3	0.323 ± 0.067	12.302 ± 3.230
K53C	19.3 ± 9.0	1.8 ± 0.6	−3.9 ± 0.8	−4.5 ± 0.8	−4.5 ± 0.8	—	—
I328C	5.1 ± 0.9	1.3 ± 0.1	−67.8 ± 6.7	−20.7 ± 2.7	−69.1 ± 6.8	0.095 ± 0.004	4.986 ± 0.426
P329C	7.2 ± 1.0	0.9 ± 0.1	−11.7 ± 1.1	−18.5 ± 1.9	−13.2 ± 1.2	0.109 ± 0.017	3.946 ± 0.579
T330C	10.2 ± 1.6	1.5 ± 0.2	−9.9 ± 2.2	−10.2 ± 2.2	−10.9 ± 2.3	—	—
I331C	19.8 ± 3.8	1.8 ± 0.2	−8.9 ± 0.8	−9.1 ± 0.8	−9.7 ± 0.8	—	—
I332C	9.6 ± 3.0	1.0 ± 0.1	−36.1 ± 11.3	−30.8 ± 9.7	−37.3 ± 11.5	0.180 ± 0.023	1.382 ± 0.248
N333C	9.2 ± 4.2	2.2 ± 1.0	−16.7 ± 2.8	−33 ± 8.3	−17.5 ± 2.9	0.191 ± 0.008	3.861 ± 0.740
L334C	9.8 ± 3.2	1.4 ± 0.3	−4.0 ± 0.9	−4.1 ± 0.9	−4.8 ± 0.9	—	—
A335C	12.1 ± 2.8	1.7 ± 0.1	−4.8 ± 1.0	−5.2 ± 1.1	−6.4 ± 1.4	—	—
T336C	25.7 ± 8.8	1.2 ± 0.2	−18.1 ± 2.5	−12.6 ± 1.7	−19.4 ± 2.5	0.090 ± 0.003	5.581 ± 0.295

All photoactive mutants were labeled in the absence of ATP, except for V48C, Q52C, K53C, N333C, and T336C, in which labeling was performed in the presence of ATP (EC_{50}). All data are mean ± SEM, n = 3–7 from at least two transfections. τ is the time constant determined at the indicated wavelength.

Table S2. Relative ion permeability for chloride

	Light-gated				ATP-gated			
Constructs	E_{rev} NaCl (mV)	E_{rev} Man (mV)	E_{rev} Na-Ise (mV)	P_{Cl}/P_{Na}	E_{rev} NaCl (mV)	E_{rev} Man (mV)	E_{rev} Na-Ise (mV)	P_{Cl}/P_{Na}
P2X2-3T	—	—	—	—	−4.3 ± 5.4	−32.5 ± 9.4	1.2 ± 5.9	0.10 ± 0.14
I328C	−1.0 ± 7.8	−38.1 ± 6.9	−2.4 ± 7.4	0 ± 0	−2.5 ± 5.9	−29.0 ± 6.1	−0.5 ± 4.6	0.09 ± 0.04
K69A/I328C	−11.8 ± 8.7	−49.0 ± 7.1	−12.9 ± 7.4	0 ± 0	—	—	—	—

Data represent mean ± SEM, n = 4–6 cells from at least two transfections. For the P2X2-3T receptor and the I328C mutant, ATP concentration was, respectively, 10 and 3 μM.

Table S3. Relative ion permeability for calcium

	Light-gated			ATP-gated		
Constructs	E_{rev} NaCl (mV)	E_{rev} Ca (mV)	P_{Ca}/P_{Na}	E_{rev} NaCl (mV)	E_{rev} Ca (mV)	P_{Ca}/P_{Na}
P2X2-3T	—	—	—	7.7 ± 3.6	9.2 ± 2.8	2.08 ± 0.22
I328C	−7.1 ± 3.2	−29.6 ± 1.9	0.56 ± 0.09	−7.2 ± 3.3	−17.9 ± 2.3	1.04 ± 0.13
K69A/I328C	0.7 ± 1.4	−27.0 ± 5.2	0.43 ± 0.09	—	—	—

Data represent mean ± SEM, n = 4–6 cells from at least two transfections. For P2X2-3T receptor and I328C mutant, ATP concentration was, respectively, 10 and 3 μM in NaCl solution. For Ca solution ATP concentration was 300 μM for both constructs.

Table S4. Relative ion permeability for NMDG

		E_{rev} NMDG (mV)			P_{NMDG}/P_{Cs}		
Constructs	E_{rev} NaCl (mV)	3 s	30 s	60 s	3 s	30 s	60 s
ATP-gated							
P2X2-3T	−9.8 ± 5.7	−73.7 ± 5.5	−60.7 ± 10.0	−49.1 ± 10.5	0.07 ± 0.01	0.12 ± 0.03	0.20 ± 0.06
Light-gated							
I328C	−5.5 ± 1.0	−58.2 ± 3.5	−50.8 ± 6.0	−54.9 ± 3.4	0.13 ± 0.02	0.17 ± 0.05	0.13 ± 0.02
K69A/I328C	1.5 ± 5.8	−52.0 ± 8.2	−56.9 ± 8.3	−59.8 ± 7.6	0.14 ± 0.01	0.12 ± 0.02	0.11 ± 0.02

Data represent mean ± SEM, n = 3–4 cells from at least two transfections. ATP concentration was 100 μM for P2X2-3T.